

## DIAMOND

### Artificially Irradiated Type IIb

Saturated blue color is rare in natural diamond, and various treatment methods have been developed to introduce or enhance this effect. The more common techniques include the annealing of type IIb diamonds under high-pressure/high-temperature (HPHT) conditions and the high-energy beam irradiation of light-colored type Ia/IIa diamonds. In the New York laboratory, we recently examined a very rare case of a type IIb diamond artificially irradiated to enhance its blue color.

This modified step-cut shield (13.70 × 10.75 × 5.09 mm) weighed 4.13 ct and was color graded Fancy Deep green-blue (figure 1). It displayed a clear color concentration in the culet, an important visual indication of artificial irradiation. Infrared absorption spectroscopy revealed a typical spectrum for a type IIb diamond, with an intense 2800 cm<sup>-1</sup> peak corresponding to an optically active boron concentration of ~40 ppb. A type IIb diamond with this size and boron concentration usually has a clear blue color (with a grayish or brownish component, depending on the intensity of plastic deformation) but not enough saturation for a Fancy Deep grade. The absorption spectrum in the UV-Vis region at liquid-nitrogen temperature showed strong GR1 absorption and a weak 666.7 nm peak, resulting in a

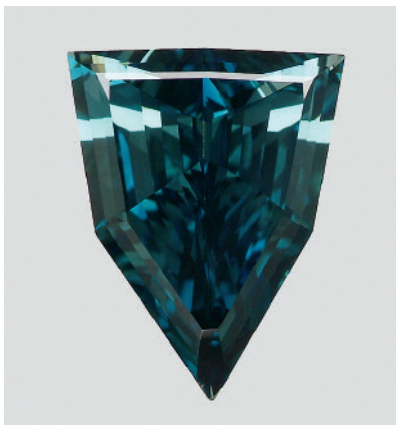


Figure 1. The Fancy Deep green-blue color of this 4.13 ct type IIb diamond is due to artificial irradiation.

transmission window in the green–light blue region. From these observations, we confirmed that this diamond had been artificially irradiated to improve its color. Strong plastic deformation indicated by high strain suggested that the diamond had a significant brown component before the treatment. This also explains the strong green coloration observed after irradiation.

Type IIb diamonds are rarely irradiated to improve their color. This unusual sample allowed us the opportunity to examine the interaction of a vacancy defect (GR1) with other defects in a type IIb diamond.

Wuyi Wang and Paul Johnson

### Type IIb Green, Natural and Synthetic

Type IIb diamonds are typically blue, resulting from boron defects, and it is very unusual to see a distinct green color in such diamonds. The New York

laboratory recently examined two type IIb green brilliants, a 5.84 ct pear shape and a 0.30 ct round, that were color graded as Fancy Dark gray-yellowish green and Fancy Light yellow-green, respectively (figure 2).

Both were very clean microscopically. In cross-polarized light, the pear showed the tatami strain typical of a natural diamond. The round brilliant did not exhibit any strain, but did show subtle color zoning (figure 3). DiamondView imaging of the pear shape revealed blue luminescence with dislocations (straight lines), indicating a natural diamond, while the round brilliant displayed a typical HPHT-synthetic growth pattern (figure 4). Spectroscopic analysis confirmed a natural color origin for the pear and an as-grown color for the round brilliant. Both were verified as type IIb by the boron bands in their mid-infrared spectra at ~2927 and ~2801 cm<sup>-1</sup>.

Dislocations in a natural diamond occur during plastic deformation, which usually creates a brown color. In type IIb diamonds, the same process adds a gray component to the blue color. In this pear-shaped stone, however, plastic deformation also contributed a yellow component. The resulting combination of yellow and blue produced the 5.84 ct diamond's yellowish green bodycolor.

Interestingly, the light yellow-green synthetic diamond had a different cause of color. In addition to boron bands, a small amount of single substitutional nitrogen was detected at 1344 cm<sup>-1</sup> in the mid-infrared spectrum. An earlier study reported mixed type IIb + Ib synthetic diamonds with blue and yellow growth sectors (J. E. Shigley et al., "Lab-grown colored diamonds from Chatham Created Gems," Summer 2004

Editors' note: All items were written by staff members of GIA laboratories.

GEMS & GEMOLOGY, Vol. 48, No. 1, pp. 47–52, <http://dx.doi.org/10.5741/GEMS.48.1.47>.

© 2012 Gemological Institute of America



Figure 2. These type IIb samples consist of a Fancy Dark gray-yellowish green natural diamond (5.84 ct, left) and a Fancy Light yellow-green synthetic diamond (0.30 ct, right).

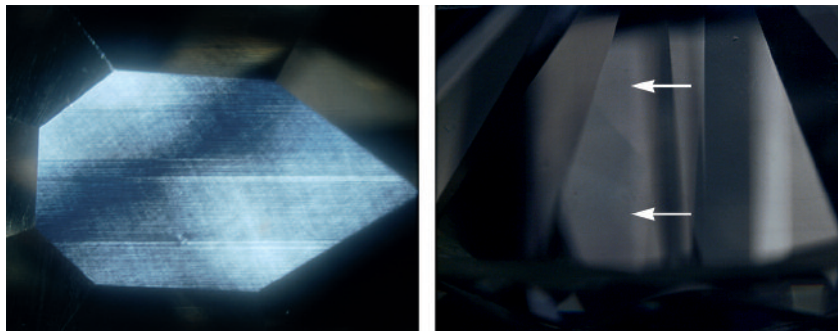


Figure 3. In cross-polarized light, the pear shape showed the tatami strain found in natural diamond (left, magnified 30×), while the synthetic round brilliant did not feature any strain but did show subtle color zoning (right, magnified 55×).

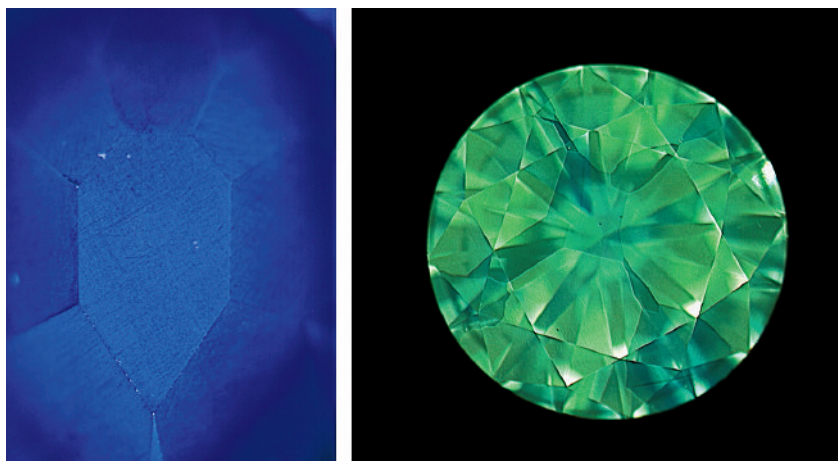


Figure 4. DiamondView imaging of the pear shape revealed blue luminescence and dislocations corresponding to a natural origin (left), while the round brilliant showed growth zoning indicative of an HPHT-grown synthetic diamond (right).

*G&G*, pp. 128–145). The article proposed that the combination of these growth sectors produced a green or grayish green color in faceted samples. In the 0.30 ct synthetic diamond reported here, the same coloring mechanism—the combined effect of a boron-dominated sector and an isolated-nitrogen sector—caused the yellow-green bodycolor. In both samples, the cutting orientation was critical to the proper mixing of the blue and yellow components. Therefore, other natural and synthetic diamonds containing blue and yellow color components may not show a green bodycolor.

These type IIb specimens demonstrate that plastic deformation or a combination of boron and nitrogen defects can result in unexpected green coloration at the hand of a skilled diamond cutter.

*Kyaw Soe Moe*

### With Unusual Color Zoning

An optical center with a broad absorption band at ~480 nm is occasionally observed in some natural yellow-orange diamonds, as well as in “chameleon” diamonds. Yet little is known about this feature’s atomic structure or its mechanism of formation in natural diamonds. In the New York laboratory, we recently encountered a particularly interesting manifestation of this optical center.

A 0.50 ct rectangular diamond (4.43 × 4.29 × 2.80 mm) was color graded Fancy Intense orange-yellow. Its absorption spectrum in the mid-infrared region showed moderate concentration of A-form nitrogen and some unassigned peaks. A strong absorption band at ~480 nm, detected in the UV-Vis spectrum at liquid-nitrogen temperature, appeared to be the cause of the intense orange-yellow color.

An outstanding feature of this diamond, visible during microscopic examination, was its distinct color zoning. The orange-yellow color was concentrated in parallel zones separated by near-colorless areas (figure 5). This banded color distribution was matched by the diamond’s fluorescence reaction to long-wave UV radiation. The orange-yellow color zones showed very strong yellow-orange fluorescence, while the

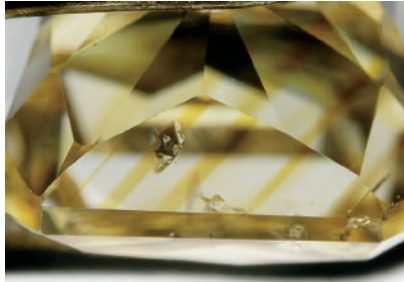


Figure 5. The orange-yellow color in this 0.50 ct diamond is concentrated in parallel zones separated by near-colorless bands.

near-colorless zones displayed strong blue fluorescence (figure 6). Microscopic observation with crossed polarizers showed little internal strain, and there was no observable strain variation between the different color zones. From these observations and the well-known fact that the 480 nm center luminesces yellow-orange to UV radiation, it became clear that the 480 nm center was distributed with a zoned structure. It was also obvious that this banded structure was not associated with plastic deformation, a very common cause of color zoning in natural diamonds.

While the origin of the unusual distribution of the 480 nm center in this diamond is unknown, the skillful orientation of the color banding by the cutter produced a face-up appearance that received a Fancy Intense color grade.

Marzena Nazz

Figure 6. When the diamond was exposed to long-wave UV radiation, the orange-yellow color zones fluoresced very strong yellow-orange, while the near-colorless zones showed strong blue fluorescence.



### Large EMERALD with Gota de Aceite Structure

*Gota de aceite* (Spanish for “drop of oil”) is a transparent angular or hexagonal growth structure rarely seen in emerald (R. Ringsrud, “*Gota de aceite*: Nomenclature for the finest Colombian emeralds,” Fall 2008 *G&G*, pp. 242–245). The New York laboratory had the opportunity to examine a 24.25 ct emerald showing this phenomenon (figure 7).

Microscopic observation revealed transparent growth structures with an oily appearance throughout the stone (figure 8, left). The effect could even be seen with the unaided eye. Some of the structures displayed six well-defined arms intercalated with six growth sectors, forming a 12-sided outline (figure 8, right); others showed an angular outline without arms. These structures occurred as individuals or in elongated groups. The c-axis of each growth structure was parallel to the optic axis of the host emerald. Such columnar growth zoning may have been developed by the parallel growth of numerous sub-crystals, which were overgrown by the host emerald (E. J. Gübelin and J. I. Koivula, *Photoatlas of Inclusions in Gemstones*, Vol. 3, Opinio Publishers, Basel, Switzerland, 2008, pp. 433–434).

The sample’s jagged two- and three-phase inclusions and spectroscopic features confirmed it was a

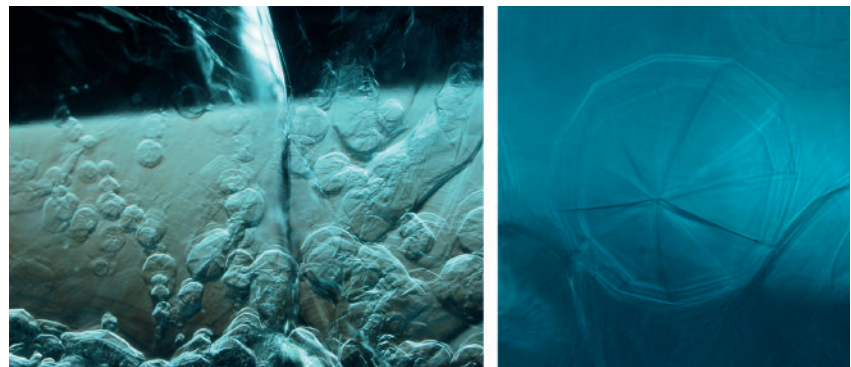


Figure 7. This 24.25 ct Colombian emerald showed the rare gota de aceite growth structure.

Colombian emerald. Individual and compact groups of colorless, transparent prismatic inclusions were identified by Raman spectroscopy as quartz (see photo in the *G&G* Data Depository at [gia.edu/gandg](http://gia.edu/gandg)), a well-known inclusion in Colombian emerald but not previously reported in *gota de aceite* specimens. The stone also contained strong planar color zoning, as well as partially healed fissures and fractures that showed evidence of clarity enhancement.

Viewed in diffused light, the emerald’s green color was clearly concentrated within the growth structures described

Figure 8. Fiber-optic illumination of the emerald clearly shows growth structures formed individually or in groups (left, magnified 25×). Some of the growth structures consist of six well-defined, intersecting arms intercalated between six growth sectors, creating a 12-sided outline (right, magnified 55×).



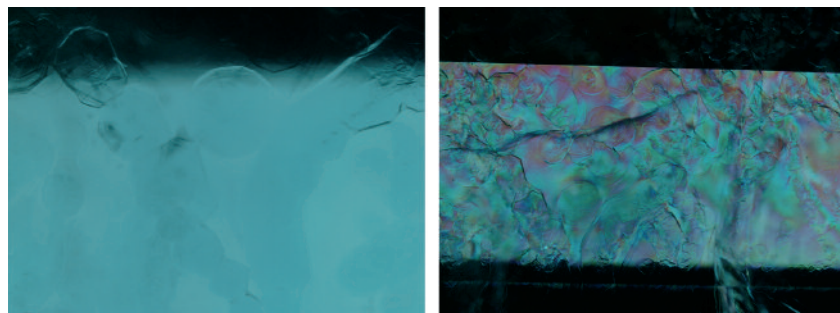


Figure 9. In diffused light, the emerald's green color was strongly concentrated in the growth structures (left, magnified 30×). The growth structures also showed high-order interference color in cross-polarized light (right, magnified 15×).

above, which also showed high-order interference colors when viewed down the optic axis in cross-polarized light (figure 9). A high-resolution UV-Vis-NIR absorption spectrum (available in the *Ge/G* Data Depository) showed broad bands at ~425 and ~613 nm, and a doublet at 680 and 683 nm; all these features are due to Cr<sup>3+</sup>. Interestingly, we also detected a very weak broad band at ~830 nm, caused by Fe<sup>2+</sup>. The presence of this band, not previously reported in Colombian emeralds, may be due to the high resolution of the spectrum.

So far, the *gota de aceite* structure has only been reported in Colombian emeralds, and thus it provides a useful tool to identify geographic origin, along with the multiphase inclusions and spectroscopic features shown by these emeralds.

*Kyaw Soe Moe and Wai L. Win*

### Update on Artificial Metallic Veining in MANUFACTURED GEM MATERIALS

A Winter 2010 Lab Note (pp. 303–304) on artificial metallic veining in composite turquoise speculated that this type of veining could appear in other gem materials. Such was the case with an interesting pair of cabochons (figure 10) that were recently examined in the Carlsbad laboratory.

The first cabochon was a 76.63 ct oval composed of white angular fragments suspended in a yellow metallic matrix. Magnification revealed cleav-

ages in the white fragments and foliated metal flakes suspended in colorless plastic (figure 11) that was easily indented by a needle and produced an acrid odor when tested with a thermal probe. Gemological testing gave spot RI readings up to 1.65 that showed a birefringence blink. The sample was inert to long- and short-wave UV radiation. Raman analysis identified the white fragments as calcite, which is consistent with the observed gemological properties. EDXRF spectroscopy revealed Cu and Zn as the dominant elements in the veins. This alloy produced an effective “gold” imitation. It is clear from the cabochon's appearance that it is intended to imitate gold-veined quartz, an attractive and rather

Figure 11. The imitation gold-in-quartz cabochon was composed of calcite veined by colorless plastic containing very fine metallic flakes consisting of copper and zinc. The foliated texture is distinctive of manufactured origin. Magnified 30×.

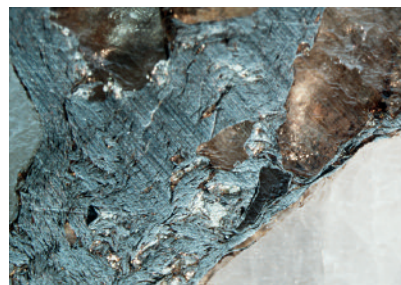


Figure 10. These 76.63 ct oval and 34.53 ct freeform cabochons proved to be manufactured composites that contain artificial metallic veining.

expensive ornamental gem material.

The second sample was a 34.53 ct green and blue freeform cabochon with copper-colored metallic veining. Magnification and Raman analysis revealed it was composed of sand-sized quartz grains suspended in a matrix of malachite, azurite, metallic flakes, and colorless plastic that also produced an acrid odor when tested with a thermal probe (figure 12). A spot RI of 1.54 was consistent with the high percentage of quartz grains present in the piece. The sample was inert to long- and short-wave UV radiation. EDXRF analysis showed that the metallic flakes were composed primarily of Cu with a small amount of Zn. A copper-colored matrix was appropriate for this imitation, considering that azurite and malachite are both copper minerals.

Figure 12. Magnification of the other cabochon shows small rounded grains of quartz suspended in a colored matrix of malachite and azurite with metallic veining. Magnified 15×.



This is the first time we have seen this manufacturing technique applied to these particular materials, and it is reasonable to assume that additional composites with artificial metallic veining could appear in a wide variety of combinations. Nevertheless, the foliated appearance of the metallic veining is quite diagnostic of manufactured origin, regardless of the component material.

*Nathan Renfro and Amy Cooper*

### Shell-Nucleated Freshwater Cultured PEARLS

In November 2011, the New York laboratory received three large flat baroque pearls for identification: one white, one orange-pink (figure 13, left), and one multicolored. They ranged from  $25.57 \times 16.16 \times 8.04$  mm to  $19.54 \times 16.44 \times 6.34$  mm. Their shapes were similar to ones we have seen in the past that were nucleated with coin- or lentil-shaped beads, first mentioned in *G&G* nearly 30 years ago (Summer 1984 Lab Notes, pp. 109–110). Both types of beads are often used for nucleation in freshwater mollusks to produce flattened cultured pearls in various shapes.

Standard gemological testing showed that all three were freshwater pearls, but X-ray images revealed an unusual internal structure (e.g., figure 13, center). All three contained what appeared to be a solid “nucleus” with distinct edges, but the outlines were not

symmetrical, or even remotely uniform. The shapes of the nuclei were clearly not natural but could not be readily identified as beads, either, due to their irregular and varied morphology.

With the client’s permission we cut open the orange-pink pearl, as its X-ray images revealed the most pronounced atypical structure, featuring one very straight edge. We sliced down the center lengthwise and found what appeared to be a roughly cut piece of shell, evidently used as the nucleus (figure 13, right). The shell nucleus had an irregular shape with some visible lustrous nacreous areas. The cross-section of the cultured pearl showed a nacre thickness ranging from ~1 to 2 mm. EDXRF spectroscopy of the shell nucleus and the surrounding nacre indicated that both were of freshwater origin, as did the strong luminescent reactions when exposed to X-rays.

While it has become more common to nucleate freshwater cultured pearls with beads, this typically involves using symmetrical pieces of shell, either round (such as those commonly used in saltwater cultured pearls) or “fancy”-shaped (as found in “coin pearls”). This is the first time we have examined freshwater cultured pearls nucleated with roughly cut shell. Using these relatively large shell nuclei produces a bigger cultured pearl in a shorter time, and the irregular shape results in a more natural baroque appearance.

*Akira Hyatt*

### Lazurite Inclusions in RUBY

The Carlsbad laboratory recently examined a large 5.09 ct unheated ruby with a noteworthy inclusion suite. Standard gemological testing gave refractive indices of 1.762–1.770 and a strong red reaction to long-wave UV radiation. Examination with a desk-model spectroscope revealed fine lines at 460, 470, and 694 nm, along with a broad absorption band centered at 560 nm, which confirmed the stone was a ruby. Microscopic examination showed dense clouds of fine iridescent rutile, unaltered protogenetic carbonates, polysynthetic twinning, and several “fingerprints.” The overall inclusion suite, combined with the strong fluorescence, suggested a low-iron, marble-hosted ruby, most likely of Burmese origin.

One particularly unusual type of inclusion stood out, however. Numerous crystallographically aligned negative crystals (see Fall 2009 Lab Notes, p. 212) were in-filled with a vibrant blue mineral that was identified by Raman analysis as lazurite (figure 14). Lapis lazuli is known to occur in Myanmar, and this geologic overlap could provide an explanation for lazurite inclusions in a corundum host.

One of these contributors (VP) saw similar blue inclusions in rubies he collected from Namya (or Nanyaseik), Myanmar, in December 2002. Analysis of a sample purchased during that trip confirmed that the inclusions (figure 15) were lazurite.

Figure 13. The orange-pink baroque cultured pearl on the left ( $25.57 \times 16.16 \times 8.04$  mm) showed an asymmetrical “nucleus” in X-ray images taken from two different orientations (center; arrows show outline of nucleus). It was sliced down its center lengthwise to reveal a roughly cut piece of shell that was apparently used as the nucleus (right).

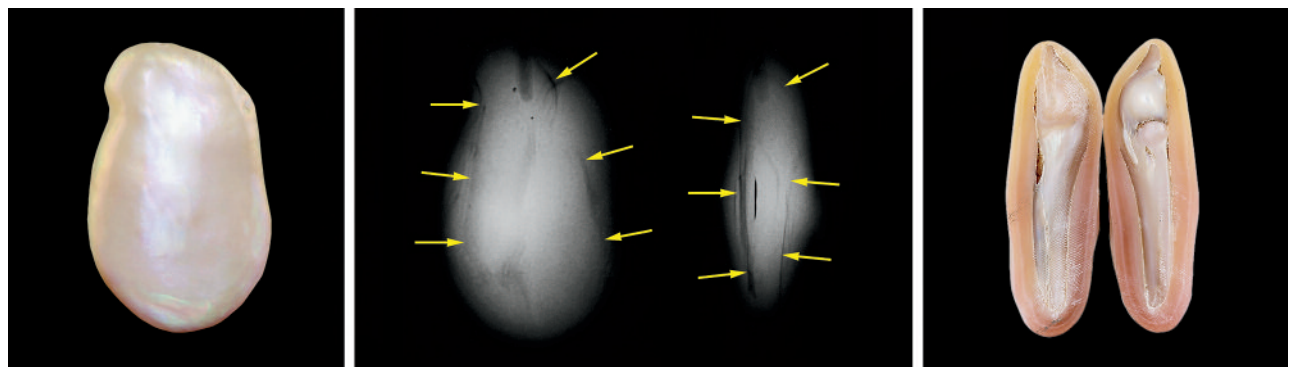




Figure 14. A 5.09 ct ruby was host to numerous lazurite-filled negative crystals. Magnified 25 $\times$ .

Blue inclusions in ruby are extremely rare, and the presence of lazurite in the 5.09 ct sample strongly supports a Burmese origin. This finding is reinforced by the other inclusions present in the stone and a low-iron composition consistent with Burmese rubies. To our knowledge, this is the first documented occurrence of inclusions of lazurite in ruby.

*Nathan Renfro and Vincent Pardieu*

### A Coated SHELL Assemblage

Whole shells are rarely submitted to GIA for identification, so the Bangkok laboratory was interested to see such a specimen recently. The specimen (figure 16) weighed 240.5 g and measured 132  $\times$  69  $\times$  56 mm. The client wanted a report identifying it as a natural seashell. Such right-handed conch shells are rare compared to left-handed varieties, and

Figure 16. This specimen (13.2 cm long) proved to consist of a natural shell that contained a filler material and was covered by an unidentified artificial coating.

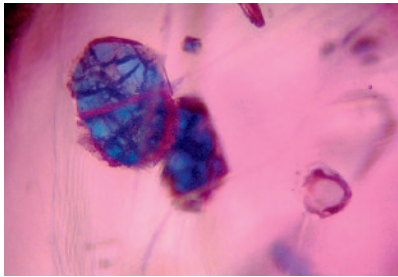
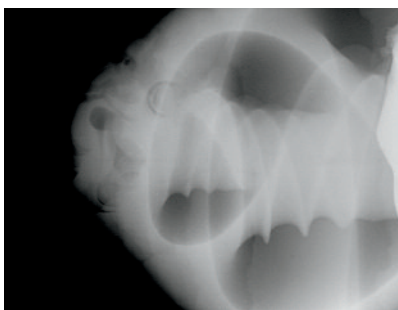


Figure 15. These blue inclusions in a 1.40 ct ruby, collected a decade ago in Namya, Myanmar, consist of lazurite-filled negative crystals similar to those in figure 14. Magnified 40 $\times$ .

they are coveted by religious devotees who consider them to be natural representations of Hindu deities.

The object did appear to be a shell, though the surface texture felt rather smooth and the piece seemed somewhat hefty for its size. Closer examination with a loupe and a gemological microscope indicated that the surface was not shell but a resinous-looking substance that contained small gas bubbles. Nor were there any obvious shell-related characteristics such as flame structure or evidence of parasite holes or channels within the shell. When exposed to long-wave UV radiation, the sample fluoresced a weak-to-moderate chalky uneven yellow rather than the more commonly encountered blue reaction, further adding to our doubts about the nature of the specimen. Raman

Figure 17. A microradiograph of the thicker end of the specimen (left image) shows the spiral shell structure and some of the filler material (whiter area on far right side). The microradiograph on the right shows part of the chamber area of the shell (A) and some of the filler used within the item (B).



analysis did not reveal the characteristic aragonite peaks at 1085 and 705/701  $\text{cm}^{-1}$  (doublet) that would be expected for most shells. EDXRF chemical analysis indicated minimal levels of calcium (the major component of any natural shell), and traces of strontium (also a common constituent of shells). Both elements should have been more prominent if the sample was a true shell.

Natural coiled gastropod shells show characteristic spiral structures when viewed in cross section or examined by microradiography. Our microradiographic examination of this object (figure 17) clearly showed the presence of natural shell with another component—most likely a filler material used to add heft. An artificial layer of material was then used to coat the assemblage and give it a realistic appearance.

This coated shell assemblage shows that even these simple religious icons may be manufactured with the intent to deceive an unsuspecting buyer.

*Nick Sturman and  
Hpone-Phyo Kan-Nyunt*

#### PHOTO CREDITS

Jian Xin (Jae) Liao—1, 2 (left), 5, 6, 7, and 13; Sood Oil (Judy) Chia—2 (right); Kyaw Soe Moe—3, 4, 8, and 9; Robison McMurtry—10; Nathan Renfro—11, 12, and 14; Vincent Pardieu—15; Nuttapol Kitdee—16; Artitaya Homkrajae—17.

